qP WAVE NUMERICAL SIMULATION IN VISCOELASTIC VTI MEDIA BY ONE-WAY WAVE EQUATION

XUE CHEN[1], LIGUO HAN[1], HELONG YANG[1] and SHUAI SHANG[2]

[1] *Jilin University, 127 Dizhigong, 938 Ximinzhu St., CHangchun, P.R. China.*
cx3141@163.com
[2] *Tarim Oilfield Ltd. CNPC, 1201 Tazhi Apt., Shishua Av., Korla, Xinjiang, P.R. China.*
shangshuai0213@163.com

(Received July 29, 2014; revised version accepted August 23, 2015)

ABSTRACT

Chen, X., Han, L., Yang, H. and Shang, S., 2015. qP wave numerical simulation in viscoelastic VTI media by one-way wave equation. *Journal of Seismic Exploration*, 24: 439-454.

Theoretical and practical studies show that the subsurface media has not only the anisotropic properties but also the anelastic properties. These properties are commonly denoted by the viscoelastic model. The conventional elastic isotropic seismic wavefield simulation could not provide sufficient foundations for the modern acquisition, processing and interpretation of the seismic data. In this article, we proposed a new qP wavefield modeling method in the viscoelastic VTI media by using the one-way wave equation. The one-way wave equation method can simulate the seismic reflection wavefield fast and accurately even in complex structure areas. The method has many advantages compared with the full-way wave equation method especially in the large-scale simulation problems, such as high calculating efficiency, low memory requirement and no interference of direct and multiple waves.

KEY WORDS: viscoelasticity, anisotropy, one-way wave equation, numerical simulation.

INTRODUCTION

The anisotropic and anelastic properties of the subsurface media are very important for the seismic data processing and interpretation. These properties have already been investigated both experimentally and theoretically by many others (i.e., Lucet and Zinszner, 1992; Lamb and Richter, 1966). Carcione (1990, 1995, 2007) studied the attenuation and quality factor in the anelastic anisotropic media and simulated the wavefield, which gave the foundation of the forward modeling in the anelastic media. The viscoelastic anisotropic media is

0963-0651/15/$5.00

a common represent of the anisotropic and anelastic media. Wu et al. (2005, 2006, 2007) studied the quasi-P wave forward modeling in viscoelastic VTI media using the finite difference method. Zhu and Tsvankin (2006) obtained the simplified attenuation anisotropic coefficients using Thomsen-style parameters by assuming the media is weakly attenuative and described the attenuation-related amplitude distortion of the plane-wave in the TI media. Guo (2007) developed the pseudo spectrum method of qP and qS wave modeling in the viscoelastic anisotropic media. Li (2011) analyzed the crosswell seismic qP wavefield in the viscoelastic VTI media using finite difference in the frequency-space domain.

The one-way wave equation method has many advantages compared with the full-way wave equation method. A variety of the one-way wave simulation methods have been developed such as the phase shift (PS) method (Gazdag, 1978), the phase shift plus interpolation (PSPI) method (Gazdag, 1984), the split-step Fourier (SSF) method (Stoffa, 1990), the Fourier finite-difference (FFD) method (Ristow, 1994) and the generalized screen propagator (GSP) method (Wu, 1994, 1997). The SSF method is suitable for the complex media and has higher calculating efficiency and more stable results compared with other methods. Based on the location principle (He et al., 1998; Xiong et al., 1998) and the geophone record theory (Xiong et al., 1999), we could use the one-way wave method to simulate the nonzero-offset seismic record. In this study, we use the SSF method to simulate the qP wavefield and analyze the effects of the anisotropy and quality factor in the viscoelastic VTI media.

THEORY

One-way wave operator for the isotropic elastic media

According to Lu (2009), the 2D homogeneous wave equation for the isotropic elastic media could be written as

$$(\partial^2 P/\partial x^2) + (\partial^2 P/\partial z^2) = (1/v^2)(\partial^2 P/\partial t^2) \quad , \tag{1}$$

where P is the seismic wavefield, x is the offset, z is the depth, v is the velocity and t is the time.

By applying 2D Fourier transformation to eq. (1) and decomposing the operators, we could obtain

$$(\partial^2 \bar{P}/\partial z^2) + [(\omega^2/v^2) - k_x^2]\bar{P} = (d^2\bar{P}/dz^2) + k_z^2\bar{P}$$

$$= [(d/dz) + ik_z][(d/dz) - ik_z]\bar{P} = 0 \quad , \tag{2}$$

where $\bar{P}$ is the 2D Fourier transformation of P, ω is the angular frequency, k_x is the horizontal wavenumber, and k_z is the vertical wavenumber.

According to the dispersion relation $k_x^2 + k_z^2 = \omega^2/v^2$, we could obtain

$$d\bar{P}/dz = \pm ik_z\bar{P} = \pm i\bar{P}\sqrt{[(\omega^2/v^2)-k_x^2]} \quad , \tag{3}$$

where a positive sign denotes the up-going wave equation and a negative sign denotes the down-going wave equation. Then the wavefield extrapolation equation is

$$\bar{P}(k_x,z_i \pm \Delta z,\omega) = \bar{P}(k_x,z_i,\omega)e^{\pm ik_z\Delta z} \quad . \tag{4}$$

The SSF method can handle the lateral velocity variation by defining a reference slowness and a perturbation in the slowness (Stoffa, 1990). The corresponding slowness at location (x,z) is $s(x,z) = 1/v(x,z)$, which can be divided into two parts:

$$s(x,z) = s_0(z) + \Delta s(x,z) \quad , \tag{5}$$

where $s_0(z)$ is the reference slowness and $\Delta s(x,z)$ is the perturbation in the slowness.

Accordingly, the extrapolation of the wavefield can be also divided into two parts. A phase shift based on the vertical wavenumber calculated by the reference slowness and a phase shift due to the perturbation in the slowness. In this case, the forward extrapolation of the wavefield could be written as follows:

$$\bar{P}(k_x,z_i \pm \Delta z,\omega) = \bar{P}(k_x,z_i,\omega)e^{-ik_{za}\Delta z} \quad , \tag{6a}$$

$$k_{za} = \sqrt{\{[\omega^2/v_0(z_i)^2] - k_x^2\}} \quad , \tag{6b}$$

$$\tilde{P}(x,z_i \pm \Delta z,\omega) = \mathrm{IFFT}[\bar{P}(k_x,z_i \pm \Delta z,\omega)]e^{-ik_{zb}\Delta z} \quad , \tag{7a}$$

$$k_{zb} = [\omega/v(x,z_i)] - [\omega/v_0(z_i)] \quad , \tag{7b}$$

where $\tilde{P}$ is the Fourier transformation of P and v_0 is the reference velocity. Here we expressed the equations using velocity instead of slowness.

Dispersion relation of viscoelastic VTI media

The stress-strain relation in elastic media is

$$T_i = C_{ij}E_j, i,j = 1,2,\cdots,6 \quad , \tag{8}$$

where T_i and E_j are the stress and strain components, respectively, and C_{ij} are the elastic moduli.

Based on the Kelvin-Voigt model, the stress-strain relation of the viscoelastic VTI media is

$$T_i = \tilde{C}_{ij}E_j = [C_{ij} + H_{ij}(\partial/\partial t)]E_j \quad , \tag{9}$$

where $\tilde{C}_{ij}$,i,j = 1,2,⋯,6 is the complex modulus which contain the viscosity H_{ij},

$$\boldsymbol{C} = \begin{bmatrix} C_{11} & C_{12} & C_{13} & 0 & 0 & 0 \\ C_{12} & C_{11} & C_{13} & 0 & 0 & 0 \\ C_{13} & C_{13} & C_{33} & 0 & 0 & 0 \\ 0 & 0 & 0 & C_{44} & 0 & 0 \\ 0 & 0 & 0 & 0 & C_{44} & 0 \\ 0 & 0 & 0 & 0 & 0 & C_{66} \end{bmatrix}, \quad \boldsymbol{H} = \begin{bmatrix} H_{11} & H_{12} & H_{13} & 0 & 0 & 0 \\ H_{12} & H_{11} & H_{13} & 0 & 0 & 0 \\ H_{13} & H_{13} & H_{33} & 0 & 0 & 0 \\ 0 & 0 & 0 & H_{44} & 0 & 0 \\ 0 & 0 & 0 & 0 & H_{44} & 0 \\ 0 & 0 & 0 & 0 & 0 & H_{66} \end{bmatrix}, \tag{10}$$

where $C_{66} = ½(C_{11} - C_{12})$, $H_{66} = ½(H_{11} - H_{12})$.

The wave equation of the viscoelastic VTI media can be obtained by using eqs. (9) and (10). By substituting the plane wave equation $u = Ue^{i(\omega t - k_x x - k_y y - k_z z)}$ into this wave equation and omitting the force item we could get the Kelvin-Christoffel equation,

$$\begin{bmatrix} G_{11}-\rho\omega^2 & G_{12} & G_{13} \\ G_{12} & G_{22}-\rho\omega^2 & G_{23} \\ G_{13} & G_{23} & G_{33}-\rho\omega^2 \end{bmatrix} \begin{bmatrix} U_x \\ U_y \\ U_z \end{bmatrix} = 0 \quad , \tag{11a}$$

$$\begin{cases} G_{11} = (C_{11} + i\omega H_{11})k_x^2 + (C_{66} + i\omega H_{66})k_y^2 + (C_{44} + i\omega H_{44})k_z^2 \ , \\ G_{12} = [(C_{11} - C_{66}) + i\omega(H_{11} - H_{66})]k_x k_y \ , \\ G_{13} = [(C_{13} + C_{44}) + i\omega(H_{13} + H_{44})]k_x k_z \ , \\ G_{22} = (C_{66} + i\omega H_{66})k_x^2 + (C_{11} + i\omega H_{11})k_y^2 + (C_{44} + i\omega H_{44})k_z^2 \ , \\ G_{23} = [(C_{13} + C_{44}) + i\omega(H_{13} + H_{44})]k_y k_z \ , \\ G_{33} = (C_{44} + i\omega H_{44})k_x^2 + (C_{44} + i\omega H_{44})k_y^2 + (C_{33} + i\omega H_{33})k_z^2 \ , \end{cases} \tag{11b}$$

where k_y is the horizontal wavenumber.

To obtain the nonzero solution of eq. (11), the Christoffel determinant must be zero:

$$\det(\mathbf{G}) = 0 \quad . \tag{12}$$

The qP wave dispersion relation of the viscoelastic VTI media can be obtained by solving eq. (12).

In order to obtain the wavefield of the qP-wave, we set the S-wave velocity $V_S = 0$ according to Alkhalifah's method (Alkhalifah, 1998, 2000) and represent the elastic modulus with the Thomsen anisotropic parameters:

$$\begin{cases} C_{11} = C_{12} = \rho(1 + 2\varepsilon)V_P^2 \ , \\ C_{13} = \rho V_P^2\sqrt{(1 + 2\delta)} \ , \\ C_{33} = \rho V_P^2 \ , \\ C_{44} = C_{66} = 0 \ , \end{cases} \tag{13}$$

where ρ is the density, V_P is the P-wave velocity, ε and δ are the Thomsen anisotropic parameters.

In a 2D situation, when $k_y = 0$, we could substitute eq. (13) into eq. (11),

$$\begin{cases} G_{11} = [\rho(1 + 2\varepsilon)V_P^2 + i\omega H_{11}]k_x^2 \ , \\ G_{13} = [\rho V_P^2\sqrt{(1 + 2\delta)} + i\omega H_{13}]k_xk_z \ , \\ G_{33} = (\rho V_P^2 + i\omega H_{33})k_z^2 \ , \\ G_{12} = G_{22} = G_{23} = 0 \ . \end{cases} \tag{14}$$

The relations between the quality factor Q and H_{ij} are

$$H_{11} = C_{11}/\omega Q, \ \ H_{13} = C_{13}/\omega Q, \ \ H_{33} = C_{33}/\omega Q. \tag{15}$$

By substituting eqs. (13), (14) and (15) into eq. (12), we could obtain the dispersion equation of the viscoelastic VTI media

$$\omega^4 = \omega^2 V_P^2(1+i/Q)[(1+2\varepsilon)k_x^2 + k_z^2] - 2(\varepsilon-\delta)V_P^4(1+i/Q)^2k_x^2k_z^2 \ . \tag{16}$$

By rewriting the above equation when $1/Q < 1$, we could get the dispersion relation:

$$k_z = \pm\sqrt{[\{(\omega/v)^4[1-i(1/2Q)]^4 - (1+2\varepsilon)(\omega/v)^2[1-i(1/2Q)]^2k_x^2\}} \\ \overline{/\{(\omega/v)^2[1-i(1/2Q)]^2 - 2(\varepsilon-\delta)k_x^2\}]} \ . \qquad (17)$$

One-way wave operator for viscoelastic VTI media

The real subsurface media exhibits both anelastic and anisotropic properties, and could not be described by the conventional wavefield extrapolation equation that we previously mentioned. To solve this problem, we introduce the qP wave dispersion relation of the viscoelastic VTI media to calculate the qP reflection wavefield.

By applying the Taylor expansion to eq. (17), and only considering the positive sign, we obtain

$$k_z^{AQ} \approx (\omega/v)[1-i(1/2Q)]\left[1+½(\eta-\xi)k_x^2/\{(\omega/v)^2[1-i(1/2Q)]^2 - \eta k_x^2\}\right] \ , \qquad (18)$$

where $\xi = 1 + 2\varepsilon$, $\eta = 2(\varepsilon-\delta)$; the superscript A and Q mean anisotropy and viscoelasticity, respectively.

Define reference velocity v_0, reference quality factor Q_a and reference anisotropic parameters ξ_0 and η_0, respectively. Then we can obtain the vertical wavenumber computed using the reference parameters:

$$k_{za}^{AQ} = \sqrt{[\{(\omega/v_0)^4[1-i(1/2Q_a)]^4 - \xi_0(\omega/v_0)^2[1-i(1/2Q_a)]^2k_x^2\}} \\ \overline{/\{(\omega/v_0)^2[1-i(1/2Q_a)]^2 - \eta_0 k_x^2\}]} \ . \qquad (19)$$

Taking the Taylor expansion to eq. (19), the phase shift due to the perturbation in the velocity and quality factor for SSF method can be obtained

$$k_{zb}^{AQ} = k_z^{AQ} - k_{za}^{AQ} \approx (\omega/v)[1-i(1/2Q)] - (\omega/v_0)[1-i(1/2Q_a)] \ . \qquad (20)$$

Substituting eqs. (19) and (20) into eqs. (6a) and (7a) we can obtain the forward extrapolation equation of the wavefield in the viscoelastic VTI media

$$\bar{P}(k_x,z_i\pm\Delta z,\omega) = \bar{P}(k_x,z_i,\omega)e^{-ik_{za}^{AQ}\Delta z} \ , \qquad (21)$$

$$\tilde{P}(x,z_i\pm\Delta z,\omega) = \mathrm{IFFT}[\bar{P}(k_x,z_i\pm\Delta z,\omega)]e^{-ik_{zb}^{AQ}\Delta z} \ . \qquad (22)$$

The interpolation method was used to handle the lateral anisotropy variation. During each depth interval Δz we chose the minimum and the maximum anisotropic parameters ξ_1 η_1 and ξ_2 η_2. We used the two groups of parameters to extrapolate the wavefield during the depth interval

$$\begin{cases} \tilde{P}(x,z_i \pm \Delta z,\omega,\xi_1,\eta_1) = e^{-ik_{zb}^{AQ}\Delta z}\, \mathrm{IFFT}\{\mathrm{FFT}[\tilde{P}(x,z_i,\omega,\xi_1,\eta_1)]e^{-ik_{za}^{AQ}(\xi_1,\eta_1)\Delta z}\} \\ \tilde{P}(x,z_i \pm \Delta z,\omega,\xi_2,\eta_2) = e^{-ik_{zb}^{AQ}\Delta z}\, \mathrm{IFFT}\{\mathrm{FFT}[\tilde{P}(x,z_i,\omega,\xi_2,\eta_2)]e^{-ik_{za}^{AQ}(\xi_2,\eta_2)\Delta z}\} \end{cases} \quad (23)$$

The final extrapolated wavefield was calculated by

$$\begin{cases} \tilde{P}_1(x,z_i \pm \Delta z,\omega) = \{[\xi_2 - \xi(x,z)]/(\xi_2 - \xi_1)\}\tilde{P}(x,z_i \pm \Delta z,\omega,\xi_1,\eta_1) \\ \qquad + \{[\xi(x,z) - \xi_1]/(\xi_2 - \xi_1)\}\tilde{P}(x,z_i \pm \Delta z,\omega,\xi_2,\eta_2) \ , \\ \tilde{P}_2(x,z_i \pm \Delta z,\omega) = \{[\eta_2 - \eta(x,z)]/(\eta_2 - \eta_1)\}\tilde{P}(x,z_i \pm \Delta z,\omega,\xi_1,\eta_1) \\ \qquad + \{[\eta(x,z) - \eta_1]/(\eta_2 - \eta_1)\}\tilde{P}(x,z_i \pm \Delta z,\omega,\xi_2,\eta_2) \ , \\ \tilde{P}(x,z_i \pm \Delta z,\omega) = [\tilde{P}_1(x,z_i \pm \Delta z,\omega) + \tilde{P}_2(x,z_i \pm \Delta z,\omega)]/2 \ . \end{cases} \quad (24)$$

NUMERICAL SIMULATION

In this study we use the nonzero-offset seismic forward modeling method which developed by He (2010, 2011) to simulate the qP wavefield in the viscoelastic VTI media. The procedures could be described as following,

1. Transform the source wavefield into the frequency-space domain using the Fourier transformation;
2. Extrapolate the source wavefield downward with the interval Δz in viscoelastic VTI media via eqs. (21), (22), (23) and (24);
3. Calculate the reflected wavefield of the current depth $\tilde{P}_r(x,z_i,\omega)$ by multiplying the extrapolated source wavefield and the reflection coefficient $r(x,z_i)$ at the same frequency in the frequency domain $\tilde{P}_r(x,z_i,\omega) = \tilde{P}(x,z_i,\omega)\cdot r(x,z_i)$;
4. Repeat steps (2) and (3) until $z = z_{max}$. Save the extrapolated source wavefield $\tilde{P}(x,z_{max},\omega)$ and reflected wavefield $\tilde{P}_r(x,z,\omega)$ for each depth;
5. Extrapolate the wavefield $\tilde{P}(x,z_{max},\omega)$ obtained from step (4) upward with interval Δz, and stack with the reflected wavefield of current depth $\tilde{P}_r(x,z_i,\omega)$ until $z = 0$;
6. Transform the extrapolated wavefield obtained from step (5) into the time-space domain by the inverse Fourier transformation to acquire the nonzero-offset seismic record.

EXAMPLES

qP wave propagation in homogeneous media

First we studied the qP wave propagation in the homogeneous media. Snapshots of the qP wavefield calculated by one-way wave equation are shown in Fig. 1. Fig. 2 shows the snapshots calculated by full-way wave equation. The S wave velocity is zero, Q = 30, $\varepsilon = 0.1$ and $\delta = 0.1$ in the model. The amplitudes of the viscoelastic case are weaker than those of the elastic case. The wavefronts are different in the isotropic media and the anisotropic media. It is round in the isotropic case, while in the anisotropic case it tends to be an ellipse.

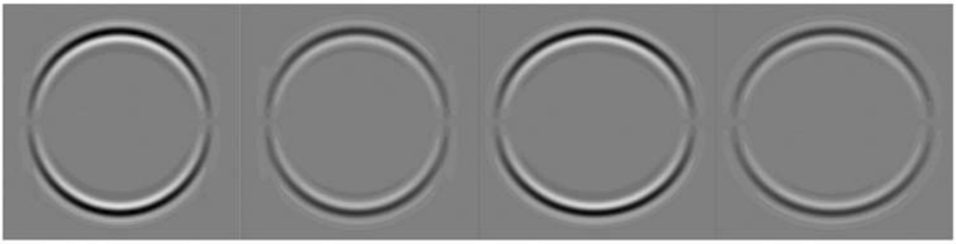

(a) (b) (c) (d)

Fig. 1. Snapshots calculated by one-way wave equation for (a) the homogeneous elastic isotropic media, (b) the homogeneous viscoelastic isotropic media, (c) the homogeneous elastic VTI media, (d) the homogeneous viscoelastic VTI media.

(a) (b) (c) (d)

Fig. 2. Snapshots calculated by full-way wave equation for (a) the homogeneous elastic isotropic media, (b) the homogeneous viscoelastic isotropic media, (c) the homogeneous elastic VTI media, (d) the homogeneous viscoelastic VTI media.

qP wavefield simulation of a horizontal layer model

We generated some synthetic qP wavefield data sets from a horizontal layer model. Fig. 3 is the schematic of the model. The parameters are listed in Table 1. Here we define three different models with different parameters. The first layer and the third layer are isotropic media with the same parameters in all the three models. The second layer of the first model is the elastic isotropic media, whereas the second and third one are the anisotropic media. The parameter Q = 10,000 means the elastic media and Q = 60 means viscoelastic media.

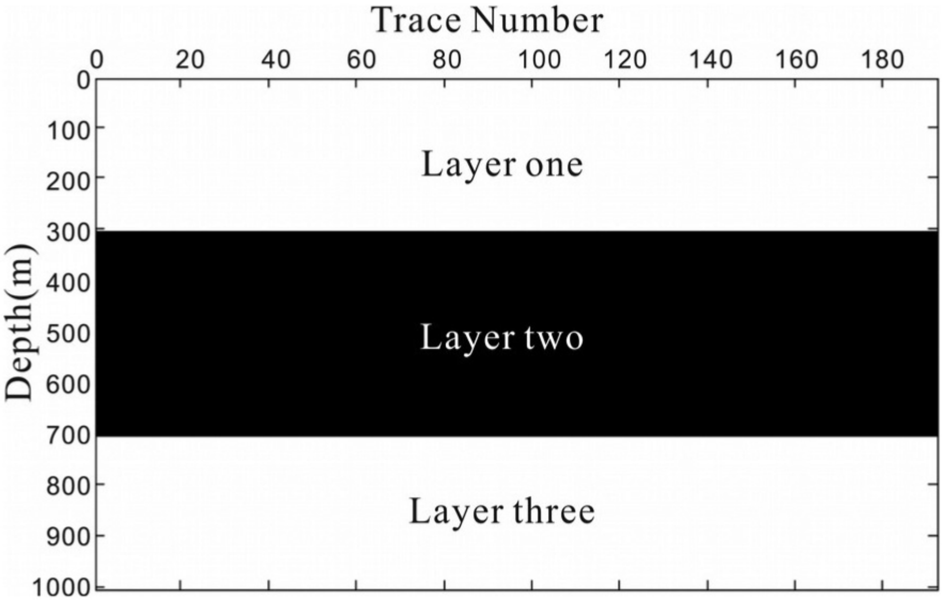

Fig. 3. The schematic of the horizontal layer model.

Table 1. The parameters of the horizontal layer model.

		v_P (m/s)	Q	ε	δ
Layer one		3000	10000	0.0	0.0
Layer two	Model 1	2700	60	0.0	0.0
	Model 2			0.4	0.2
	Model 3			-0.1	-0.2
Layer three		3000	10000	0.0	0.0

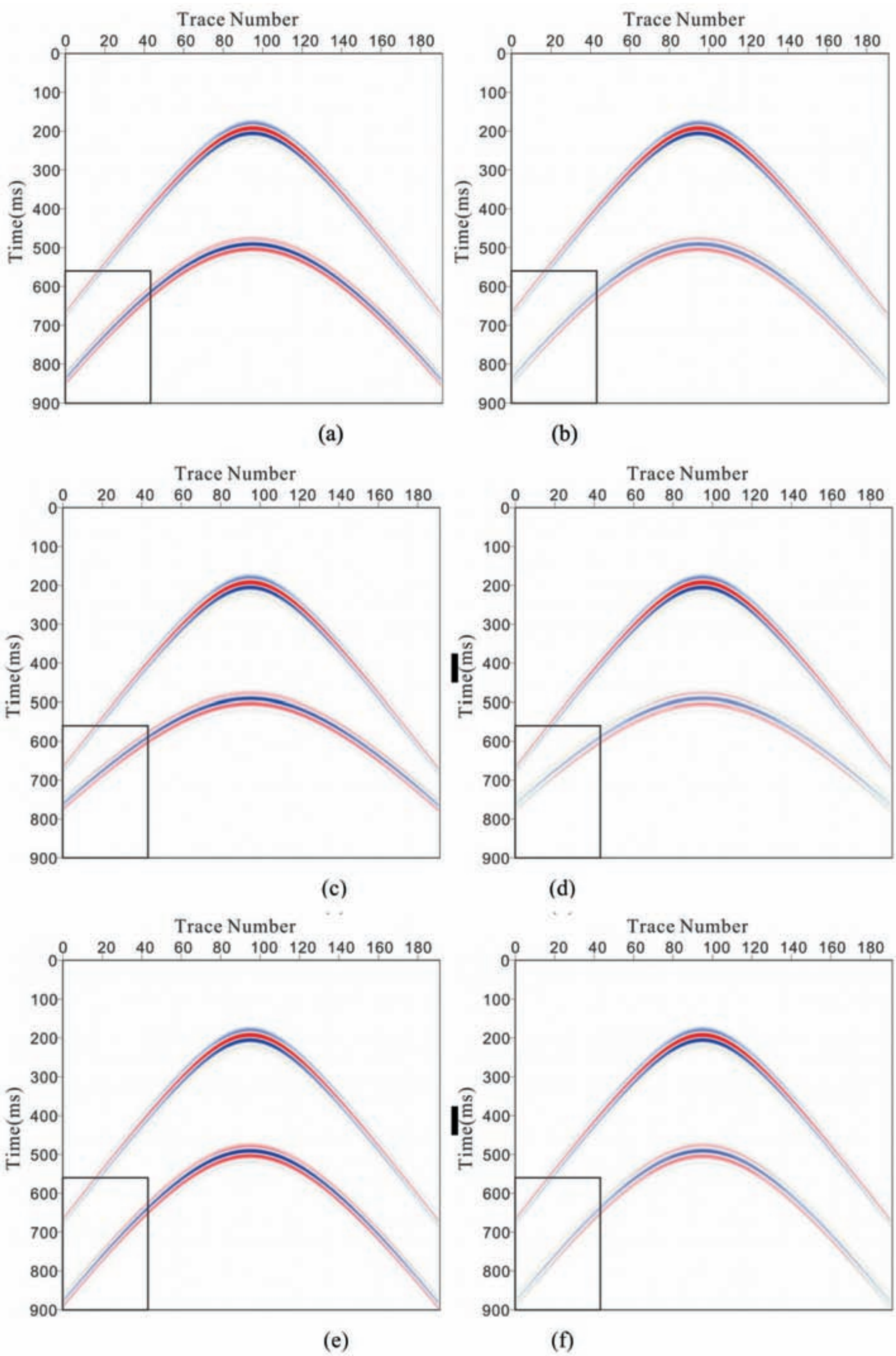

Fig. 4. The qP wavefield synthetic shot records of (a) Model 1 without attenuation; (b) Model 1 with attenuation; (c) Model 2 without attenuation; (d) Model 2 with attenuation; (e) Model 3 without attenuation; (f) Model 3 with attenuation.

The synthetic seismic records of the three models with and without attenuation are shown in Fig. 4. The source is located in Trace No. 96. Comparing Figs. 4(a) and 4(b), we could find that the energy of the second reflection is weak and the amplitude is reduced due to the attenuation of the viscoelastic isotropic media. A similar pattern is shown in Figs. 4(c), (d), (e) and (f). We have also found that the traveltime in the anisotropic media is different from that in the isotropic media. The magnitude of the change is controlled by the anisotropic parameters. When ε and δ are both positive, the qP wave with the nonzero incident angle propagates faster in the anisotropic media than in the isotropic media. As a result, the nonzero offset travel time is shorter in the anisotropic situation. In contrast, when ε and δ are both negative, the nonzero offset travel time is longer in the anisotropic situation than in the isotropic situation. We should also note that in the actual subsurface media ε is usually positive.

The normalized spectra of the central trace reflections of the second interface are shown in Fig. 5. We could find that the attenuation laws in isotropic and anisotropic situations are consistent, i.e., the high frequency energy is absorbed, the amplitude is reduced, the dominant frequency becomes lower, and the frequency bandwidth becomes narrower.

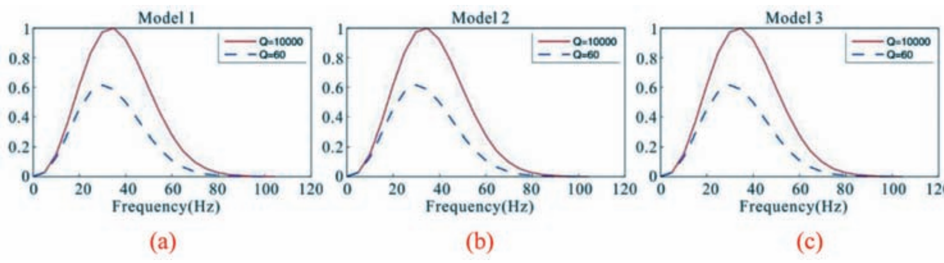

Fig. 5. Corresponding second reflection normalized spectrums of Fig. 4: (a) Model 1; (b) Model 2; (c) Model 3.

Fig. 6 shows the extracted central trace and two different offset traces in each of the six synthetic shot records in Fig. 4. Black lines represent the results without attenuation, and gray lines represent the results with attenuation. The solid lines represent the results of Model 1, the dashed lines represent the results of Model 2, and the dash-dot lines represent the results of Model 3. The amplitude reduction due to the absorption of the viscoelastic media and the travel time variation caused by the anisotropy can be clearly observed. It is shown that the effect of the anisotropy becomes more obvious with the increasing offset.

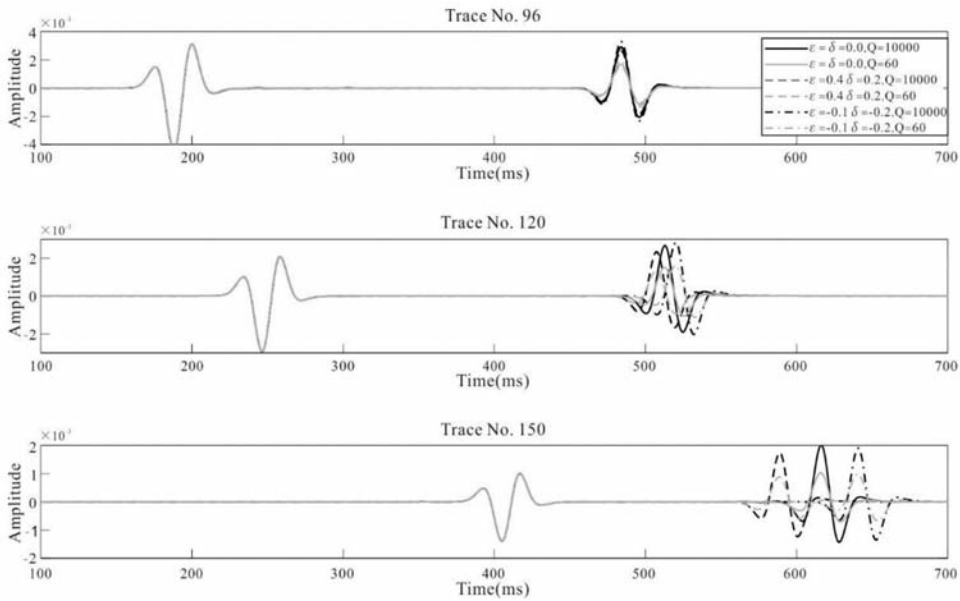

Fig. 6. The central traces (Trace No. 96) and two different offset traces (Trace No. 120, Trace No. 150) of the synthetic shot records shown in Fig. 4.

qP wavefield simulation of Hess VTI model

We applied our method to the Hess VTI model (HESS) with the parameters shown in Fig. 7. We used a smaller version of this model and set a quality factor for it. Note that the quality factor may not be realistic here and we used it to test our method.

Fig. 8 shows the qP wavefield synthetic shot records of the Hess VTI model under different situations. The source is located in the trace No. 175. We could find that the four shallow reflections in Figs. 8(a) and 8(c) are exactly the same. However, the deep reflections energy is weaker in Fig. 8(c) than that in 8(a) as the result of attenuation. The same conclusions can be obtained from Figs. 8(b) and 8(d). As shown in Figs. 8(a), (b), (c) and (d), we could find that the travel times are different at nonzero offset due to the anisotropy. Because the anisotropic parameters ε and δ are both positive, the nonzero offset travel times of the reflections in the anisotropic media is shorter than that in the isotropic media. This makes the anisotropic reflections a little more flat and the changes are more obvious at the large offset.

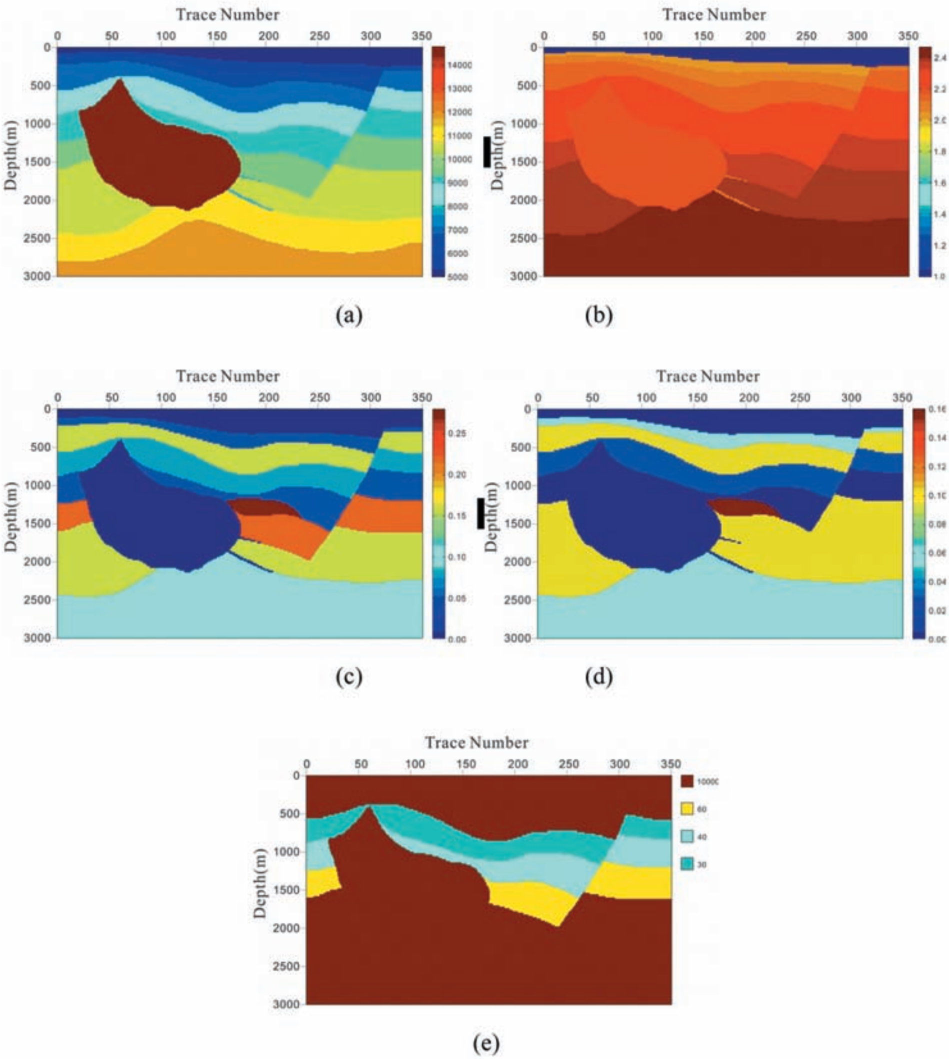

Fig. 7. Different parameters of the Hess VTI model. (a) P wave velocity, (b) density, (c) anisotropic parameter ε, (d) anisotropic parameter δ, (e) quality factor.

CCONCLUSION

Viscoelasticity and anisotropy can better characterize the subsurface media. In this study, we proposed a new qP wave numerical simulation method in the viscoelastic VTI media based on the one-way wave equation. The method is suitable for the complex media and can calculate the qP reflection wavefield fast and accurately. We also analyzed the propagation of qP wave in the viscoelastic VTI media by generating some synthetic data sets based on our modeling method. The results show that the seismic wave propagation in the viscoelastic anisotropic media is much different from that in the elastic isotropic media. First, due to the high frequency energy absorption of the subsurface media, the amplitude and dominant frequency of the seismic wave is reduced and the frequency bandwidth becomes narrower. Second, the nonzero offset travel time of the seismic wave changed because of the effect of the anisotropy, when ε and δ are both positive, it is reduced, when ε and δ are both negative, it is increased, and the effects become more obvious for far offsets data.

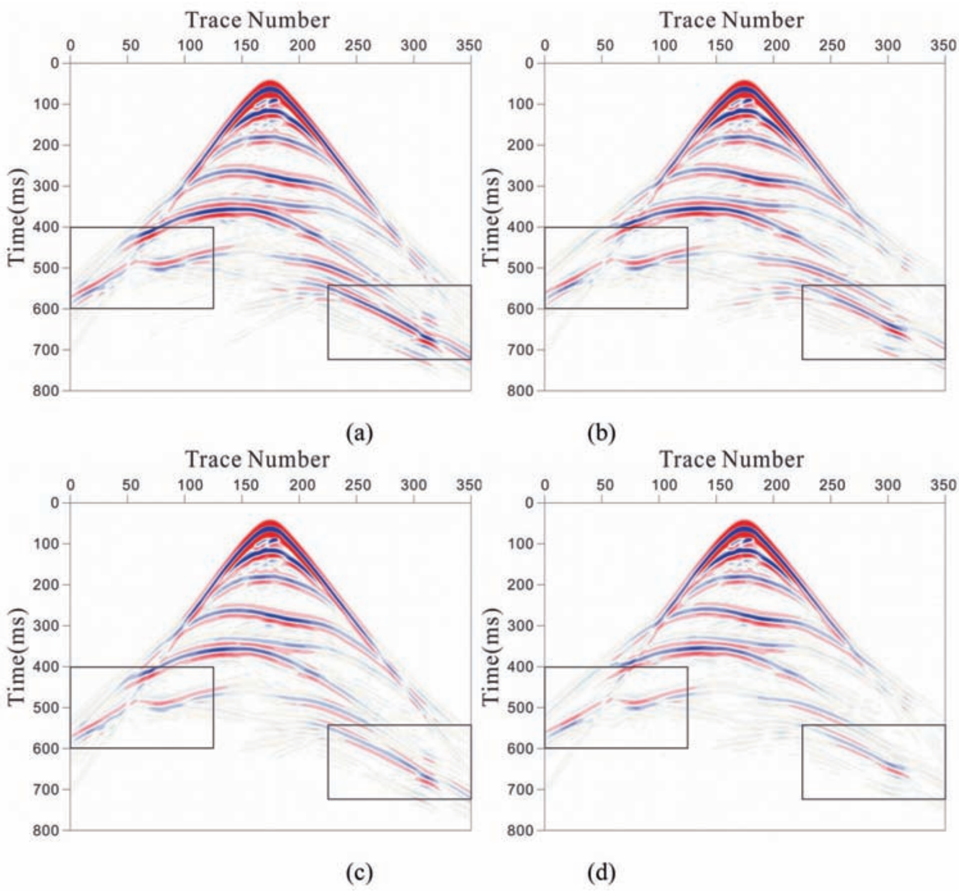

Fig. 8. The qP wavefield synthetic shot records of the Hess VTI model under different situations. (a) Isotropic media without attenuation, (b) anisotropic media without attenuation, (c) isotropic media with attenuation, (d) anisotropic media with attenuation.

ACKNOWLEDGEMENTS

We would like to thank the National Science and Technology Major Project of China (No.2011ZX05025-001-07) for the funding support. And we are really grateful to Yun Long and Wubing Deng for the help during the research.

REFERENCES

Alkhalifah, T., 1998. Acoustic approximations for processing in transversely isotropic media. Geophysics, 63: 623-631.

Alkhalifah, T., 2000. An acoustic wave equation for anisotropic media. Geophysics, 65: 1239-1250.

Carcione, J.M., 1990. Wave propagation in anisotropic linear viscoelastic media: Theory and simulated wavefields. Geophys. J. Internat., 101: 739-750.

Carcione, J.M., 2007. Wave Fields in Real Media: Wave propagation in anisotropic, anelastic, porous and electromagnetic media, 2nd Ed. Elsevier Science Publishers, Amsterdam.

Carcione, J.M. and Cavallini, F., 1995. Attenuation and Quality Factor Surfaces in Anisotropic-viscoelastic Media. Mechanics of Materials, 19: 311-327.

Gazdag, J., 1978. Wave equation with phase shift method. Geophysics, 43: 1342-1351.

Gazdag, J. and Sguazzero, P., 1984. Migration of seismic data by phase shift plus interpolation. Geophysics, 49: 124-131.

Guo, Z.Q., Liu, C., Yang, B.J., Liu, Y. and Wang, D., 2007. Seismic wavefields modeling and feature in viscoelastic anisotropic media. Progress in Geophysics (in Chinese), 22: 804-810.

He, B.H., 2011. The study of numerical simulation of seismic wave in attenuation medium and extraction of absorption properties. M.Sc. thesis, China University of Petroleum, Qingdao.

He, B.H. and Wu, G.C., 2010. Seismic attenuation modeling based on one-way wave equation (in Chinese). Chin. Geophys. Soc. Ann. Mtg.: 654-654.

He, Z.H., Xiong, G.J. and Zhang, Y.X., 1998. Nonzero offset seismic forward modeling by one way acoustic wave equation. Expanded Abstr., 68th Ann. Internat. SEG Mtg., New Orleans: 1921-1924.

Lamb, J. and Richter, J., 1966, Anisotropic acoustic attenuation with new measurements for quartz at room temperature. Proc. Roy. Soc. London, Ser. A, 293: 479-492.

Li, G.H., Feng, J.G. and Zhu, J.M., 2011. Quasi-P wave forward modeling in viscoelastic VTI media in frequency-space domain. Chin. J. Geophys., 54: 200-207.

Lu, J.M. and Wang, Y.G., 2009. The Principle of Seismic Exploration (in Chinese). China University of Petroleum Press, Dongying.

Lucet, N. and Zinszner, B., 1992. Effects of heterogeneities and anisotropy on sonic and ultrasonic attenuation in rocks. Geophysics, 57: 1018-1026.

Ristow, D. and Rühl, T., 1994. Fourier finite-difference migration. Geophysics, 59: 1882-1893.

Stoffa, P.L., Fokkema, J.T. and de Luna Freire, R.M. and Kessinger, W.P., 1990. Split-step Fourier migration. Geophysics, 55: 410-421.

Wu, G.C. and Liang, K., 2005. Quasi P-wave forward modeling in frequency space domain in VTI media. Oil Geophys. Prosp. (in Chinese), 40: 535-545.

Wu, G.C., 2006. Seismic wave propagation and imaging in anisotropy media (in Chinese). China Univ. of Petroleum Press, Dongying.

Wu, G.C. and Liang, K., 2007. High precision finite difference operators for qP wave equation in VTI media. Progr. in Geophys. (in Chinese), 22: 896-904.

Wu, R.S., 1994. Wide-angle elastic wave one-way propagation in heterogeneous media and an elastic wave complex-screen method. J. Geophys. Res., 99(B1): 751-766.

Wu, R.S. and Jin, S., 1997. Windowed GSP (generalized screen propagators) migration applied to SEG-EAEG salt model data. Expanded Abstr., 67th Ann. Internat. SEG Mtg., Dallas: 1746-1749.

Xiong, G.J., He, Z.H., Huang, D.J., Zhang, Y.X., Jiang, S.R. and Yan, P., 1998. Improved positioning principle of forward modeling. Oil Geophys. Prosp., 33: 742-748.

Xiong, G.J., He, Z.H., Huang, D.J., Zhang, Y.X., Jiang, S.R. and Zhuo, B.H., 1999. Geophone downward principle of CSP record forward simulation. Geophys. Prosp. for Petrol., 38(2): 43-49.

Zhu, Y. and Tsvankin, I., 2006. Plane-wave propagation in attenuative transversely isotropic media. Geophysics, 71(2): T17-T30.